

Accepted Manuscript

Title: Mesoporous silica as phase transfer agent in the biphasic oxidative cleavage of alkenes using triazole complexes of ruthenium as catalyst precursors

Authors: L. Leckie, S.F. Mapolie

PII: S0926-860X(18)30379-X
DOI: <https://doi.org/10.1016/j.apcata.2018.07.038>
Reference: APCATA 16764

To appear in: *Applied Catalysis A: General*

Received date: 27-3-2018
Revised date: 24-7-2018
Accepted date: 26-7-2018

Please cite this article as: Leckie L, Mapolie SF, Mesoporous silica as phase transfer agent in the biphasic oxidative cleavage of alkenes using triazole complexes of ruthenium as catalyst precursors, *Applied Catalysis A, General* (2018), <https://doi.org/10.1016/j.apcata.2018.07.038>

This is a PDF file of an unedited manuscript that has been accepted for publication. As a service to our customers we are providing this early version of the manuscript. The manuscript will undergo copyediting, typesetting, and review of the resulting proof before it is published in its final form. Please note that during the production process errors may be discovered which could affect the content, and all legal disclaimers that apply to the journal pertain.



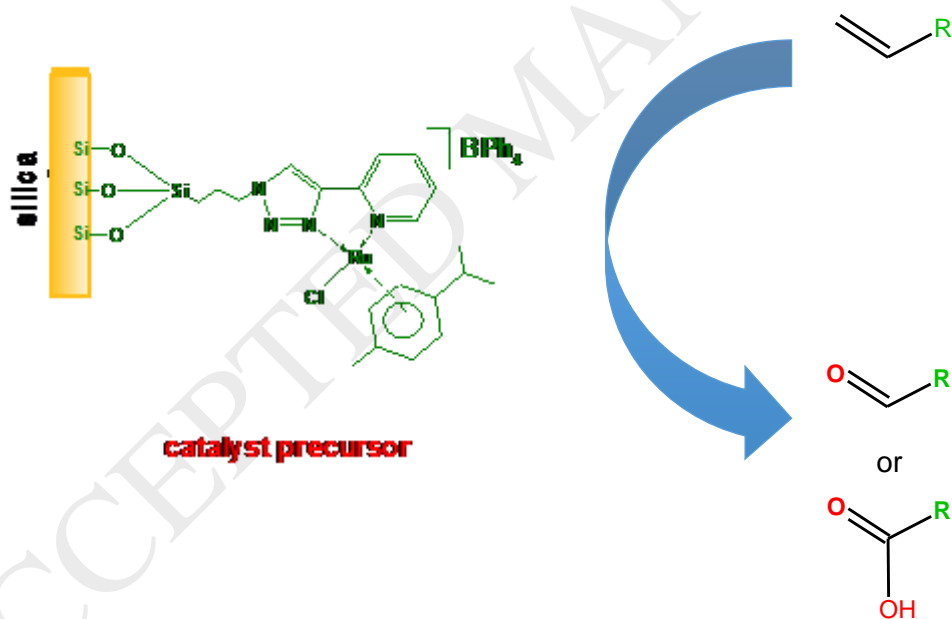
Mesoporous silica as phase transfer agent in the biphasic oxidative cleavage of alkenes using triazole complexes of ruthenium as catalyst precursors

L. Leckie ^a, S.F. Mapolie ^{a,*}

^a DST-NRF Centre of Excellence in Catalysis (c*change), Department of Chemistry and Polymer Science, Stellenbosch University, Private Bag 1, Matieland, 7601 Stellenbosch, South Africa.

*Corresponding author: smapolie@sun.ac.za (S.F. Mapolie)

Graphical abstract



Highlights

- A series of novel ruthenium complexes of pyridine-triazole and quinoline-triazole ligands were immobilized on mesoporous silica, MCM-41 and SBA-15.
- The immobilized catalysts were shown to be highly active in the oxidative cleavage of alkenes using $\text{IO}(\text{OH})_5$ as oxidant.
- The silica supports acts as phase transfer agents to transport catalyst precursors from organic layer to aqueous layer.
- High selectivity to the aldehyde product is observed for all the catalyst precursors at short reaction times.

Abstract

The oxidative cleavage of alkenes was performed using ruthenium triazole-arene complexes immobilized on mesoporous silica materials. These silica-organometallic hybrid materials were found to show enhanced activity when compared to conventional homogeneous systems even when operating at a relatively low catalyst loading. The enhanced catalytic performance of these heterogeneous systems can be attributed to the mesoporous silica acting as a phase transfer agent in the biphasic catalyst system.

Keywords

Immobilized complexes, mesoporous silica, oxidative cleavage of alkenes, ruthenium-arene complexes

1. Introduction

Unsaturated hydrocarbons, such as alkenes can be converted to more valuable oxygenates via oxidative cleavage of the carbon-carbon double bond. This is a useful synthetic process and has been the topic of several reviews [1–5]. Oxidative cleavage of olefins is often performed industrially employing non-catalytic processes such as ozonolysis. There are also other stoichiometric reactions involving transition metal based oxidation reagents such as KMnO_4 or CrO_2Cl_2 . The latter is known to selectively transform olefins into aldehydes or carboxylic acids. The use of such systems is however undesirable due to the toxic nature of the metal salts employed and the fact that the organic substrates are usually not very soluble in the aqueous medium required for the permanganate ion [5].

Catalytic olefin oxidations using a transition metal catalyst, often based on group 7 or 8 metals, and in conjunction with oxidants, such as IO_4^- or H_2O_2 have been investigated as alternatives [5,6]. Ruthenium, osmium, and tungsten catalysts have previously been reported to catalyze the oxidative cleavage of various unsaturated fatty acids and alkenes. In addition Fe and Mn based catalytic systems have also been reported. However, these are usually limited to activated alkenes, such as styrene. Alkenes can selectively be cleaved to form aldehydes using osmium-based catalysts with NaIO_4 as an oxidant. A major drawback however is that many of the Os compounds are often toxic, which make their usage not desirable [5]. Over recent years, ruthenium-based catalysts have gained increasing interest due the versatility of the metal oxide, RuO_4 , which has been shown to be the active species in these oxidative alkene cleavage reactions. Ruthenium tetroxide has been employed stoichiometrically in the oxidation of alkenes to aldehydes [5]. There are several reports where even ruthenium trichloride on its own has simply been employed to catalytically convert alkenes into carboxylic acids [7,8] in the presence of an oxidant such as sodium hypochlorite or sodium periodate [9,10]. Ruthenium trichloride in the presence of periodic acid, $\text{IO}(\text{OH})_5$, is known to convert alkenes to carboxylic acids however in this case the reduction product, HIO is very soluble in water alleviating problems during the work-up of the reaction [5]. Studies have shown that RuO_4 exhibits high selectivity towards terminal oxygenated cleavage products. This is due to the fact that neither dihydroxylated nor epoxidized intermediates are involved in the reaction mechanism using these types of catalysts [11]. The primary products are aldehydes with carboxylic acids obtained as a result of over-oxidation of the aldehyde [5]. Due to the chemoselectivity of the Ru catalysts for terminally functionalized oxygenates, there have been several attempts to develop new ruthenium-based catalysts. Some reports on the development of homogeneous and heterogeneous ruthenium based catalytic systems for the oxidative alkene cleavage reaction have appeared in the recent literature. For example, Shoair et al. discovered that a Ru-bipy complex in the presence of $\text{IO}(\text{OH})_5$ oxidatively cleaved both terminal and internal alkenes to yield carboxylic acids [9]. These authors also found that the incorporation of a bidentate nitrogen donor ligand such as bipyridine, led to a catalyst capable of mediating the oxidative cleavage reaction at a much lower (tenfold lower) catalyst loading than other ruthenium catalyst precursors, which do not possess a nitrogen donor ligand.

In light of these developments, our group has recently embarked on a study to investigate the ability of other N,N chelating ligands to mediate the Ru catalyzed oxidative cleavage of alkenes. Recently we reported enhanced activity for the complexes based on pyridine-imine as well as quinoline-imine ligands [12]. In the same publication, further enhancement in activity and selectivity was observed when these complexes were immobilized on mesoporous silica supports. We have now elaborated on these systems exploring the use of other complexes of Ru using novel nitrogen-based chelating ligands. The current work is thus an attempt at exploring the use of pyridine-triazole, pyridine-N-oxide/triazole as well as quinoline-triazole complexes of ruthenium in oxidative cleavage reactions. Both homogeneous as well as immobilized complexes of this type were evaluated as catalyst precursors.

2. Experimental

2.1. General remarks and instrumentation

All reactions were performed using standard Schlenk techniques under an inert atmosphere (Argon or Nitrogen) unless stated otherwise. Highly air-sensitive materials were stored in a nitrogen-purged glovebox and all manipulations with these materials were carried out in the glovebox to prevent decomposition or oxidation. In the case of microwave-assisted reactions, a CEM Discover SP Microwave reactor was used. Fourier transform infrared (FT-IR) spectra were recorded using an ATR accessory on a Nicolet Avatar 330 FT-IR spectrometer equipped with a Smart Performer ATR attachment with a ZnSe crystal. NMR spectra were recorded on a Varian Unity Inova instrument at 300, 400 and 600 MHz for ^1H and ^{13}C NMR spectroscopy. ESI-MS was performed using a Waters Synapt G2 Mass Spectrometer. A Thermo Elemental Analyzer (CHNS-O) was used for the accurate determination of the elemental composition of samples. BET nitrogen adsorption/desorption analysis was done on a Micromeritics 3Flex Surface Characterization instrument (77 K). The samples were degassed at 273 K for 18 hours prior to analysis. Powder XRD analysis was done using a BRUKER AXS (Germany) D8 Advance Diffractometer. Transmission electron micrographs were collected using an FEI Tecnai G2 20 field-emission gun (FEG) TEM, operated in bright field mode at an accelerating voltage of 200 kV, on a Ni/Cu grid. Energy dispersive X-ray spectra were collected using an EDAX liquid nitrogen cooled Lithium doped Silicon detector. A TA Instruments Q500 thermogravimetric analyser was used to acquire TGA data. ICP-OES analysis was performed on a Spectro Arcos ICP-OES with a Burgener T2100 and cyclonic spray chamber as nebulizer. The samples were prepared by digesting between 20-30 mg of the immobilized catalyst in concentrated nitric acid (15 ml), at 100 °C for 24 hours. The sample was then filtered and made up to a known volume and analyzed. A Radleys 12-stage carousel parallel reactor equipped with a gas distribution system was used for the catalytic reactions. GC analyses were performed using a Varian 3900 instrument equipped with a polar Cyclosil-B column (30 m, 0.250 mm diam. and 0.25 μm film) using helium as carrier gas. *p*-xylene was used as internal standard. HPLC-MS analyses were performed on a Waters Synapt G2 instrument fitted with an Acquity BEH C18 2.1 x 50mm 1.7 μm column. ESI mass spectra were recorded by direct injection into a stream of acetonitrile and 0.1% formic acid employing a cone voltage of 15 V on a Waters API Quattro Micro spectrometer.

2.2. Materials

All reagents were acquired from Sigma-Aldrich or Fluka and used without any further purification. These include 2-ethynyl pyridine, 2-chloroquinoline, copper iodide, octyl bromide, 3-chloropropyl triethoxysilane, *meta*-Chloroperoxybenzoic acid (mCPBA), α -terpinene, $\text{RuCl}_3 \cdot x\text{H}_2\text{O}$, cetyltrimethylammonium bromide (CTAB), tetraethyl orthosilicate (TEOS) and Poly(ethylene)-*block*-poly(propylene)-*block*-poly(ethylene). All solvents were purchased from Sigma-Aldrich or Kimix

Chemicals. dichloromethane, diethyl ether, hexane, toluene and tetrahydrofuran were purified using a Pure SolvTM Micro solvent purifier fitted with activated alumina columns. Ethanol and methanol were purified by distillation over a mixture of magnesium filings and iodine. Acetonitrile was purified by distillation over phosphorous pentoxide. CCl₄ was used without further purification.

2.3 Synthesis of model and functionalized ligands and complexes

See Supplementary Information for experimental details and characterization of the model and siloxane functionalized ligands and complexes.

2.4 Synthesis of immobilized catalysts IC1-IC6

The native silica, MCM-41 [13] and SBA-15 [14], were synthesized according to modified literature procedures. The procedure for immobilization of the siloxane-functionalized complexes on mesoporous silica, MCM-41 and SBA-15, as well as the characterization of these materials is discussed in the Supplementary Information but follows a previously published approach for other ruthenium complexes [12].

2.5 Typical procedure for the oxidative cleavage of alkenes

The catalyst, **MC1** (5×10^{-4} mmol), was added to a mixture of CCl₄ (1.25 mL) and MeCN (1.25 mL) in a Radley's parallel reactor tube. To the yellow mixture was added the appropriate alkene (0.5 mmol) followed by a solution of oxidant, IO(OH)₅, (0.57 g, 2.5 mmol) dissolved in distilled water (2.5 mL). The biphasic reaction mixture was allowed to stir for the required time at 25 °C. The mixture was then extracted with diethyl ether (9 mL) and the organic layer dried over anhydrous MgSO₄. The mixture was sampled (1 mL) and *p*-xylene (0.100 mL) added as internal standard for product quantification. Conversions were determined via gas chromatography. The work-up of the reaction mixture for the oxidative cleavage of cyclopentene was different to that of 1-octene and styrene. In the case of cyclopentene as substrate, the mixture was extracted with DCM and the organic layer dried over MgSO₄, 1 mL of the organic fraction was sampled for GC analysis. The solvent was then removed from the aqueous layer remaining to obtain a white residue. MeCN (~ 5ml) was added to the white residue at which point a large amount of the white solid remained undissolved. The mixture was syringe filtered. The filtrate was dried over MgSO₄ and 1 mL was sampled for GC analysis.

2.6. UV-Vis investigation to probe the formation of RuO₄ in the oxidative cleavage of 1-octene

Reactions were carried out under the general reaction conditions employed for the oxidative cleavage of 1-octene in the absence of substrate. At the appropriate time between 0.2-0.4 ml of the organic layer of the reaction was sampled and this was then diluted to a total volume of 3 ml with a 1:1 (v/v) MeCN/CCl₄ solvent mixture. The UV-Vis spectra of these solutions were recorded over the wavelength range 200 nm to 800 nm.

2.7. Reaction of model complex, MC2, with periodic acid, with the aim of identifying possible reaction intermediates in the oxidative cleavage reaction

Model complex, **MC2**, (20 mg, 0.02 mmol) was dissolved in MeCN (1 ml). To the golden yellow solution was added IO(OH)₅ (27 mg, 0.12 mmol) dissolved in water (0.25 ml). The solution turned dark brown within 30 min and a small amount of brown precipitate formed. The mixture was filtered through cotton wool and celite, to afford a golden yellow filtrate. The celite had been discoloured to brown. The solvent was removed at 35 °C from the filtrate to obtain a golden yellow residue.

3. Results and Discussion

3.1 Synthesis of ruthenium triazole arene pre-catalysts

Prior to the immobilization of the ruthenium triazole-arene complexes, we prepared the siloxane functionalized precursors as well as the corresponding unfunctionalized model complexes by reacting the [Ru(*p*-cymene)Cl₂]₂ dimer with the appropriate N,N or N,O ligand in a 1:2 mole ratio respectively (Scheme 1). The immobilization of the different complexes is effected by simple condensation of the siloxane functionalities with the silanol groups on the surface of the silica support. This is illustrated for immobilized catalysts, **IC1** and **IC2** in Scheme 2. The full range of immobilized catalyst systems prepared is illustrated in Chart 1. Also shown are the corresponding model complexes. For complete details of the preparation of the precursor complexes, consult the Supporting Information.

The immobilized catalysts were characterized using a range of solid state analytical techniques including infrared spectroscopy, nitrogen adsorption/desorption (BET) surface analysis, low-angle powder X-ray diffraction, transmission electron microscopy (TEM), scanning electron microscopy (SEM), thermal gravimetric analysis (TGA) and ICP-OES. TEM, SEM and powder XRD results confirm that very little change in the morphology of the support is observed after immobilizing the catalysts. The TEM micrographs of the immobilized catalysts **IC1** (immobilized on MCM-41) and **IC2** (immobilized on SBA-15) are shown in Figure S62† and Figure S63† (ESI) respectively. These compare well with what has been previously been observed for types of mesoporous silica materials [15,16]. The immobilization of the complexes onto the supports was also confirmed by the decrease in surface area as determined by means of BET (Brunauer Emmett Teller) surface analysis. In all cases, Type IV isotherm plots [17-20] were obtained for the MCM-41 and SBA-15 based immobilized catalysts (Figure S70† and Figure S71†, ESI respectively), confirming the mesoporous nature of the materials. The surface area, pore diameter and total pore volume for MCM-41 based materials and SBA-15 based materials calculated from BET analysis are summarized in Table 1. The results correspond well with

those reported previously [21-24]. Immobilization of the complexes onto the supports was also confirmed by the increase in weight loss relative to the native silica obtained from TGA analysis and the detection of ruthenium on the supports (Figures S66† and S67†, ESI)

3.2 Oxidative cleavage of alkenes

The model and immobilized catalysts depicted in Chart 1 were evaluated in the oxidative cleavage of various alkenes.

3.2.1 Oxidative cleavage of 1-octene

The model complexes (**MC1-MC3**) and immobilized ruthenium complexes (**IC1-IC6**) were employed in the oxidative cleavage of 1-octene (Scheme 3) in the presence of periodic acid as oxidant. The catalysis was performed in a biphasic solvent mixture consisting of an aqueous phase and an organic phase of acetonitrile and carbon tetrachloride. The former being a coordinating solvent is required to prevent the formation of insoluble ruthenium intermediates during the catalytic process [10a] while the latter has been reported to play a role in solubilisation of the *in-situ* formed RuO₄, which is generally regarded as the active species [10b]. Other water immiscible solvents, including other chlorinated solvents were either themselves susceptible to oxidation or gave little to no conversion of substrates. The catalysts were found to successfully transform 1-octene to heptaldehyde and subsequently to heptanoic acid, with the latter only being formed over extended reaction times. From these results, it is clear that one can selectively produce aldehydes by simply controlling the reaction time. The efficiency of the various catalysts were compared against each other, in terms of turnover numbers (TON's) at various reaction times (Table 2). Also shown are turnover frequencies (TOF's), which gives some insight into catalyst life times.

When comparing the model and immobilized catalyst systems, we see that all the immobilized catalysts were significantly more active than their model counterparts when used at similar metal concentrations. The immobilized catalyst systems gave good conversions at a relatively low metal concentration of 0.1 mol%. This trend can for example be seen for the pyridine triazole N,N system where the TON's obtained for immobilized catalysts, **IC1** and **IC2**, are significantly greater than the those obtained for the model complex, **MC1** (entries 1-6, Table 2). This phenomenon is also observed for the pyridine-N-oxide/triazole (**IC3** and **IC4**) and quinoline-triazole (**IC5** and **IC6**) catalyst systems,

although in the case of the pyridine-N-oxide/triazole the difference in activity between the model and the immobilized catalyst is less pronounced. It should be emphasized that the activities were compared at the same metal loading and under similar reaction conditions. It is thus obvious that immobilization significantly enhances the efficacy of the catalysts. The mode by which this enhancement occurs is discussed later (*vide infra*).

Another observation that is evident from the results, is that the N,O (pyridine-N-oxide/triazole) catalyst systems, model complex (**MC2**) and immobilized complexes (**IC3** and **IC4**) were more effective in the oxidative cleavage reaction than the N,N systems viz. the pyridine-triazole complexes (**MC1**, **IC1** and **IC2**) and quinoline-triazole complexes (**MC3**, **IC5** and **IC6**). Thus for example the pyridine-N-oxide/triazole model complex, **MC2**, achieved a reasonable TON of 250 compared to the model N,N systems, **MC1** and **MC3**, which showed TON's of only 48 and 92 respectively, when employing these catalyst at the same ruthenium concentration over a 3 hour reaction time. The immobilized analogues of the pyridine-N-oxide/triazole catalyst was also more active than the immobilized pyridine-triazole and quinoline-triazole analogues with the catalyst containing the pyridine-N-oxide moiety achieving turnover numbers, which are almost double those for the other two N,N complexes. All the immobilized catalysts, achieve conversions between 90-100% after about 9 hours reaction time. The homogeneous model complexes on the other hand with the exception of **MC2**, show conversions of only 6-24% over a longer reaction time (~12 hour). **MC2**, which is the complex with a pyridine-N-oxide moiety, shows a 100% conversion after about 6 hours reaction time. However, in this particular case the reaction solution at this stage contains a mixture of aldehyde and carboxylic acid unlike the case for immobilized analogues (**IC3** and **IC4**) which show 100% selectivity towards the carboxylic acid at shorter reaction times. Another noticeable observation is the fact that the immobilized catalysts shows an activity profile which appears relatively stable over extended time. This is evident when looking at the TOF values for these catalyst systems. The model complexes, **MC1** and **MC3** show a significant decrease in TOF values over time, which is indicative of a dramatic decrease in the concentration of active species in solution over time. The immobilized analogues on the other hand display relatively steady TOF values indicating the steady generation of active species over extended times.

3.3. Investigation into reaction pathway using immobilized catalyst systems

Having observed that the immobilized catalysts performed significantly better than their model counterparts (Table 2) it was decided to investigate this in more detail.

3.3.1. Detection of the active species by UV-vis spectroscopy

Previous reports in the literature including work from our own group, indicate that the oxidative cleavage of alkenes using Ru based catalysts is in fact mediated by RuO₄, which is formed *in-situ* during the reaction [9, 19, 25]. For the previously reported systems, the presence of RuO₄ in the reaction

mixture could be confirmed using UV-Vis spectroscopy. The presence of RuO_4 is indicated by two characteristic absorption bands, one between 280-340 nm and the other in the region between 370-420 nm (Figure 1). In addition, these peaks also possess a distinctive fine structure [12,16]. These characteristic peaks are also observed in reaction mixtures in which our immobilized catalysts had been treated with the oxidant, $\text{IO}(\text{OH})_5$. (Figures 1 and 2) The concentration of this species was found to be higher in solutions of those complexes which gave higher TON's in the catalytic reactions.

3.3.2. Possible mechanism

Based on previous reports, a probable mechanism for the oxidative cleavage reaction is shown in Scheme 4. A crucial step in the cycle involves the transformation of the ruthenium precursor to RuO_4 in the presence of the oxidant, periodic acid. As indicated earlier, UV-Vis experiments confirm that the Ru (II) complex is indeed the source of the tetroxide. It is proposed that the alkene substrate subsequently coordinates to the RuO_4 to form a ruthenium (VI) diester [12]. Unfortunately, in our case the metal diester intermediate was not detected in reactions using our catalyst precursors. However, this is possibly due to the fleeting nature this species. Although such metallo-diester species are widely accepted as an important intermediate in these reactions, its detection has only been reported once previously. Albarella *et al.* reported the detection of traces of such a metallo-diester when carrying out a stoichiometric reaction between RuO_4 and (-)- α -pinene performed in CCl_4 [11]. To the best of our knowledge, this is the only example where this type of particular metallo-ester has been detected. Currently it is accepted that the rearrangement of this cyclic ruthenium diester ultimately affords the aldehyde as product in conjunction with RuO_2 . The latter is then oxidized in the presence of oxidant to reform RuO_4 . The aldehyde product formed initially, can subsequently undergo further oxidation to the analogous carboxylic acid product [12]. This second oxidation process is however much slower, resulting in the carboxylic acid product only being observed at extended reaction times. The re-oxidation of RuO_2 is a well-known reaction and is regarded a simple REDOX reaction. It has been invoked as a crucial step in the oxidative alkene cleavage in several reports in the literature [5, 10a, 10b and 10e].

The immobilized triazole-based complexes reported in this paper were found to be effective catalysts in the oxidative cleavage of alkenes giving high conversions at a relatively low catalyst loading of 0.1 mol%. This is at much lower metal loading than conventional systems. For example the well-known and widely employed Sharpless catalyst system give high conversions but requires catalyst loadings around 2 mol% [10a]. A report by Yang *et al.* in which the oxidative cleavage of alkenes using RuCl_3 are reported uses Ru loading of 3.5% [10c]. The use of RuO_2 as a catalyst precursor has also been reported but once again high metal concentrations are required to ensure reasonable conversion of the substrate [10d]. Homogeneous systems supported by other N,N chelating ligands have been reported before and gave reasonable yield working at 0.5 mol % metal loading [9]. This however is five times higher than the catalyst loading for our catalyst system.

3.3.3. Role of the mesoporous silica support on the catalytic process

From the results obtained during our catalytic studies, it is clear that the support has a significant impact on the catalytic activity. It was initially thought that the silica played a role in stabilizing the active oxidizing species, RuO_4 , and in so doing ensured a reasonable concentration of this species present in solution resulting in faster conversion of the substrate when using the immobilized systems. However closer investigation of this system, revealed that the enhanced activity is in fact not due to catalyst stabilization by the support but rather that another phenomenon was at play. What we noticed was that during the execution of the oxidative cleavage reactions with immobilized catalysts, **IC1-IC6**, the supported catalysts displayed some hydrophilic-like characteristics in that almost all of the silica material migrates to the water layer of the biphasic reaction mixture. On reflection, this is not entirely unexpected as silica with its high concentration of silanol groups on its surface can reasonably be expected to show some degree of hydrophilicity. Indeed scanning the literature, we came across some reports related to this phenomenon [27-30]. Included amongst these are few instances where silica has been employed as a support in biphasic catalysis and where it facilitates phase transfer of a catalyst between two immiscible solvents [33]. However, to the best of our knowledge, this has not previously been reported for biphasic oxidative cleavage of alkenes.

3 depicts how the mesoporous silica, MCM-41 migrates to the aqueous phase in biphasic mixtures. In mixture **1**, we see that native MCM-41 prefers the aqueous phase (lower layer) to the organic layer (diethyl ether) on top. Mixture **2** shows that the model complex **MC1** dissolved in the organic phase in a mixture of $\text{CCl}_4/\text{MeCN}/\text{H}_2\text{O}$, whereas in mixture **3** we see that immobilized analogue **IC1** migrates to the aqueous layer in the same solvent mixture. Finally, in mixture **4** we observe that native MCM-41 also prefers the aqueous phase in the $\text{CCl}_4/\text{MeCN}/\text{H}_2\text{O}$ solvent system. Taking the above observations, into consideration, it becomes apparent that the enhanced catalytic performance seen for the immobilized complexes can largely be attributed to the hydrophilic nature of mesoporous silica. This allows the silica-supported catalysts to be easily transported to the aqueous phase. In the case of the immobilized catalysts, this facilitates the transfer of the ruthenium complex, immobilized on the silica, from the organic CCl_4/MeCN phase into the aqueous phase in which the oxidant, $\text{IO}(\text{OH})_5$, is present. This ensures close contact between the ruthenium pre-catalyst and the oxidant in the aqueous layer, thus promoting the formation of the active species, RuO_4 . The latter is insoluble in water but highly soluble in CCl_4 . It therefore rapidly migrates back to the organic phase where it comes into contact with the hydrocarbon substrate. The silica is thus acting as some sort of phase transfer agent. In contrast, in the cases where pure model homogeneous complexes are used, the complexes are soluble in the organic phase (CCl_4/MeCN), and therefore the ruthenium pre-catalyst only comes into contact with the water

soluble $\text{IO}(\text{OH})_5$ at the interface of the aqueous and organic layers. In this case, a far lower concentration of the catalyst precursor is exposed to the oxidant, resulting in a much lower rate of formation of RuO_4 (**Error! Reference source not found.4**).

When comparing the different types of support it can be seen that the SBA-15 based systems are slightly more active than their MCM-41 counterparts. This is most likely due to the fact that SBA-15 has larger pore sizes than MCM-41. Assuming some of the catalyst precursors in addition to being on the surface of the support are also encapsulated in the pores, it would be reasonable to suggest that access by the oxidant to the encapsulated metal sites would be easier in the case of the larger sized SBA-15. This would enhance rate at which the active species is generated.

Finally given the nature of the reaction where the Ru precursor is ultimately converted into soluble RuO_4 , we decided not to embark on any recycling experiments.

3.3. *Oxidative cleavage of other alkenes with immobilized catalyst, IC4*

With an effective catalyst system in hand, the most active of the immobilized catalysts, **IC4**, was applied in the oxidative cleavage of other alkenes to assess the substrate scope of the immobilized ruthenium pyridine-triazole based catalyst. Thus the oxidative cleavage of styrene (Scheme 5) and cyclopentadiene (Scheme 5) was investigated using the above complex as catalyst precursor.

Table 3 shows that selective and complete conversion of the styrene to form benzaldehyde occurs within a 30-minute reaction time. Over-oxidation to benzoic acid could only be observed if the reaction was allowed to proceed for 1 hour. However, the oxidation of benzaldehyde to benzoic acid seems to be a much slower process, with only 6.6% selectivity for benzoic acid being observed after a reaction period of 1 hour.

We also evaluated the oxidative cleavage of a cyclic alkene, viz. cyclopentene. In the case of the oxidative cleavage of a cyclic olefin, it can be expected that the reaction would result in the formation of the corresponding bifunctional aldehyde and/or carboxylic acid (Scheme 6). This is indeed what was observed in our system, where glutaraldehyde and glutaric acid were obtained as products after the oxidative cleavage of cyclopentene using **IC4** (Entries 3 and 4, Table 3). In addition to the bifunctional acid and aldehyde, an intermediary, namely 5-hydroxypentanoic acid, was identified as a product using HPLC-MS (Fig. S7†) Complete conversion of the substrate could be observed after a relatively short reaction time of only 30 minutes, with glutaraldehyde as the only product. When the reaction time was extended to 1 hour, the selectivity changed such that a mixture of glutaraldehyde, 5-hydroxypentanoic acid and glutaric acid could be observed in the product stream. When comparing the oxidative cleavage of the various substrates, we see that in the case of the oxidation of 1-octene, around only 50% of the substrate was converted predominantly into the heptaldehyde after 3 hours. However, for the activated alkenes such as styrene and cyclopentene, the cleavage reaction proceeded much faster, resulting in

100% conversion of the substrate into the aldehyde product within 30 minutes. This shows that the immobilized catalyst **IC4** can effectively be used for the selective conversion of different types of alkenes into valuable oxygenated products.

3.4 Probing the catalyst behavior of the ruthenium triazole model complexes

To further understand the behavior of these ruthenium pre-catalysts in the alkene oxidative cleavage, we employed the model complexes, **MC1** and **MC2**, to investigate how these are converted into the active species, RuO_4 . The role of the ligands in this process was also examined. UV-vis spectroscopy was used to probe this.

3.4.1. Monitoring the transformation of the catalyst precursor into RuO_4 using UV spectroscopy

The first point of departure was to detect the formation of ruthenium tetroxide in reactions in which the above-mentioned model complexes are treated with oxidant. As expected, the analysis of these mixtures was not straightforward due to the fact that some of the major peaks in the UV-Vis spectrum of the model complex (pre-catalyst) overlap with those of RuO_4 . This results in the latter only being detected once enough of the model complex had been transformed in the presence of the oxidizing agent. In light of this, the rates of RuO_4 formation from the model catalysts could not be compared directly with those obtained for the immobilized catalysts. The UV-vis spectra of reaction mixtures obtained of the model catalysts in the presence of the oxidant are depicted below in Figure 5. The UV-vis spectra of the pure model complexes, **MC1-MC3** show peaks between 250-270 nm associated with electronic transitions in the ligand. We also see metal to ligand charge transfer (MLCT) bands between 285-300 nm and 310-370 nm for complexes **MC1** and **MC3**. These two complexes are supported by chelating N,N chelating ligands, *viz.* pyridine-triazole (**MC1**) and quinoline-triazole (**MC3**). The UV-vis spectrum of **MC2**, a complex that has a chelating ligand, which incorporates a pyridine-N-oxide moiety, does not show any distinct metal to ligand charge transfer band. A band around 400 nm, associated with the d-d transitions of the metal ion, can be observed for all three model complexes.

When the model complexes are exposed to the oxidant, we see a transformation in the spectra of all three pre-catalysts. The appearance of a medium intensity peak between 290-320 nm and a low intensity peak between 380-400 nm can be associated with the formation of ruthenium tetroxide. The latter peak is however somewhat masked by the signal for the d-d transitions of the metal ion. The transformation of model catalyst **MC2** to RuO_4 occurs over a relatively short period (5-hour), whereas for the model catalyst systems, **MC1** and **MC3**, we only detect RuO_4 at much longer reaction times (~24 hours). Thus it is clear that the pyridine-N-oxide moiety of **MC2** facilitates the formation of RuO_4 . In contrast, the precursors with N,N chelating systems (**MC1** and **MC3**) are less able to do so. It is thought that in the case of the pyridine-N-oxide complexes, the N-oxide functionality facilitates the transfer of the oxo group to metal centre leading to the formation ruthenium oxide species. This type of oxygen atom transfer process is not unusual and has been observed for late transition metal complexes. Thus,

for example Mei et al. proposed such an oxygen atom transfer process from coordinated pyridine-N-oxide ligands to the metal in their study of catalytic C-H functionalization using mediated by iron complexes [34]. Similar oxygen transfer atom reactions were investigated computationally by Pardue et al. for Fe, Ru and Os complexes [35].

3.4.2. Activation of model ruthenium pre-catalyst, **MC2**

To further probe the behaviour of the catalyst precursor **MC2**, in solution, we reacted it with the oxidant, periodic acid, with the aim of identifying the type of species present in solution. **MC2**, was dissolved in MeCN and reacted with 5 mol equivalents of periodic acid dissolved in a small amount of water. The mixture, which changed colour from golden yellow to brown almost immediately, was filtered and the solvent removed from the filtrate to afford a brown residue. The residue was analysed using proton NMR spectroscopy, FT-IR spectroscopy, ESI mass spectrometry, as well as thin layer chromatography (TLC) in order to gain an understanding of the species being formed during the reaction. One of the products detected, was the free pyridine-N-oxide/triazole ligand, albeit in a relatively small amount. This was confirmed by TLC analysis using an authentic sample of the ligand. Furthermore the crude mixture was also analysed by ESI mass spectrometry as well as proton NMR spectroscopy. In addition to the free ligand, the proton NMR spectrum (Fig. S5†) shows the presence of a ruthenium complex in which a pyridine-triazole ligand (7.11-7.71 ppm) as well as the *p*-cymene ligand (5.43-5.69 ppm) are both co-ordinated to the ruthenium centre i.e. a metal complex resembling the model complex **MC1**, which contains a pyridine-triazole ligand.

This is confirmed by ESI mass spectrometry (Figure 6) of the crude reaction mixture which show a peak at m/z : 529.17 corresponding to this species. Also detected in the MS is a peak corresponding to some unreacted pyridine-N-oxide/triazole model complex **MC2** (m/z : 545.16). In addition a signal assigned to the free pyridine-N-oxide/triazole ligand (m/z : 275.19) is also seen in the spectrum. A high mass signal at m/z : 621.10 can be assigned to an analogue of the pyridine-triazole model complex **MC1** in which the original chloride is substituted by an iodide as an inner sphere ligand. The source of iodide is believed to be the oxidant, $\text{IO}(\text{OH})_5$, which is thought to be reduced to the iodide ion during the reaction. An important difference between the pyridine-triazole and pyridine-N-oxide/triazole complexes employed as catalysts in this reaction, is that the complex containing the pyridine-N-oxide moiety, **MC2**, has a bidentate ligand with an oxygen donor site, the origin of which is the pyridine-N-oxide functionality. In this case, oxygen transfer from the N-oxide to the metal centre is an important step. As was seen previously in the proposed mechanism for oxidative alkene cleavage (Scheme 4), the transfer of oxygen atoms from an oxidant to ruthenium centre plays a crucial role in the formation of the metal tetroxide. Therefore, the presence of an oxygen atom already coordinated to the metal centre,

as is the case in complex **MC2** could facilitate oxygen transfer to the metal and thus accelerate the formation of RuO_4 . This possibility does not exist for the simple pyridine-triazole complex **MC1**. In the case of the **MC2** system, transfer of the oxide ion from the pyridine-N-oxide/triazole ligand to metal would result in the formation of the N, N pyridine triazole ligand. The transformation of the pyridine-N-oxide/triazole complex **MC2** to the pyridine triazole complex **MC1** is indeed what was observed as evidenced from mass spectral and ^1H NMR analysis. This then suggests that there is facile oxygen atom transfer from the pyridine-N-oxide/triazole ligand to the ruthenium centre when **MC2** is employed as catalyst precursor. This allows the pyridine-N-oxide containing complexes to mediate the oxidation process more effectively.

4. Conclusion

The model ruthenium catalysts (**MC1-MC3**) and immobilized analogues (**IC1-IC6**) employed in the oxidative cleavage of 1-octene promoted the formation of heptaldehyde and heptanoic acid as products. The immobilized catalysts were more active than their model counterparts at a relatively low catalyst loading of 0.1 mol%. The pyridine-N-oxide/triazole catalysts showed enhanced activity when compared with the N,N (pyridine -triazole and quinoline-triazole) catalysts. UV-Vis studies confirmed RuO_4 to be an important intermediate in the catalytic cycle in reactions for both the model and immobilized catalyst systems. The immobilized catalysts were hydrophilic in nature, the result being that the immobilization of the ruthenium complex on the silica support facilitates the transfer of the ruthenium pre-catalyst from the organic phase to the aqueous phase, which contains the oxidant. This promotes the oxidation of the precursor to RuO_4 , which is the actual active species. This phase transfer allows the proposed active species, RuO_4 , to form at a faster rate leading to an overall enhancement of reaction rates for the immobilized catalysts compared to their model analogues. The immobilized catalyst **IC4** was capable of the oxidative cleavage of other alkenes such as styrene and cyclopentene where the catalyst selectively afforded the aldehyde products benzaldehyde and glutaraldehyde, respectively, at shorter reaction times (0.5 hrs).

Investigation into the transformation of the pyridine-N-oxide model complex, **MC2** in the presence of oxidant, periodic acid, showed the formation of a complex with an N, N chelating ligand. This suggests that oxygen atom transfer from the pyridine-N-oxide/triazole ligand to the ruthenium centre is most likely occurring when **MC2** is employed as catalyst precursor in the oxidative cleavage of alkenes. The oxygen atom transfer from a pyridine-N-oxide moiety of the ligand in the case of **MC2** is the likely reason why this pre-catalysts showed superior catalytic activity compared to the N,N complexes, **MC1** and **MC3**.

5. Acknowledgements

The authors acknowledge the financial support by the National Research Foundation (NRF), grant no. GUN 90493 and the c*change Centre of Excellence in Catalysis, the Department of Science and Technology (DST), South Africa. The Division of Research Development at Stellenbosch University is also thanked for their financial support.

ACCEPTED MANUSCRIPT

References

- 1 A. Rajagopalan, M. Lara and W. Kroutil, *Adv. Synth. Catal.*, 2013, 3321–3335.
- 2 S. N. Dhuri, K. Cho, Y. Lee, S. Y. Shin, J. H. Kim, D. Mandal, S. Shaik and W. Nam, *J. Am. Chem. Soc.*, 2015, **137**, 8623–8632.
- 3 T. Naota, H. Takaya and S. Murahashi, *Chem. Rev.*, 1998, **98**, 2599–2660.
- 4 V. Piccialli, *Molecules*, 2014, **19**, 6534–6582.
- 5 P. Spanning, P. C. A. Bruijninx, B. M. Weckhuysen and R. J. M. Klein Gebbink, *Catal. Sci. Technol.*, 2014, **4**, 2182–2209.
- 6 A. Haimov, H. Cohen and R. Neumann, *Interface*, 2004, 11762–11763.
- 7 R. Neumann and C. Abu-gnim, *Chem. Commun.*, 1989, 1324–1325.
- 8 W. P. Griffith, A. G. Shoair and M. Suriaatmaja, *Synth. Commun.*, 2000, **30**, 3091–3095.
- 9 A. G. F. Shoair and R. H. Mohamed, *Synth. Commun.*, 2006, **36**, 59–64.
- 10 (a) P. Carlsen, T. Katsuki, V. Martin and K. Sharpless, *J. Org. Chem.*, 1981, **46**, 3936–3938.
(b) K. Kaneda, S. Haruna, T. Imanaka, K. Kawamoto. *J. Chem. Soc. Chem. Commun.* 1990, 1467-1468. (c) D. Yang, C. Zhang, *J. Org. Chem.* 2001, **66**, 4814-4818. (d) H. Okumoto, K. Ohtsuka, S. Banjaya, *Synlett.* 2007, **20**, 3201–3205. (e) S. Wolfe, S. K. Hasan and J. R. Campbell, *J. Chem. Soc. D*, 1970, 1420.
- 11 L. Albarella, F. Giordano, M. Lasalvia, V. Piccialli and D. Sica, *Tetrahedron Lett.*, 1995, **36**, 5267–5270.
- 12 H. Kotzé and S. Mapolie, *Appl Organometal Chem*, 3643. 2017;31:e3643.
<https://doi.org/10.1002/aoc.3643>
- 13 Q. Cai, W.-Y. Lin, F.-S. Xiao, W.-Q. Pang, X.-H. Chen and B.-S. Zou, *Microporous Mesoporous Mater.*, 1999, **32**, 1–15.
- 14 D. Zhao, Q. Huo, J. Feng, B. F. Chmelka and G. D. Stucky, *J. Am. Chem. Soc.*, 1998, **120**, 6024–6036.
- 15 V. Meynen, P. Cool and E. F. Vansant, *Microporous Mesoporous Mater.*, 2009, **125**, 170–223.
- 16 A. Taguchi and F. Schüth, *Microporous Mesoporous Mater.*, 2005, **77**, 1–45.
- 17 Balbuenat P.B. & Gubbins K.E., *Langmuir*, 1993, **9**, 1801–1814.
- 18 H. Zhang, J. Sun, D. Ma, X. Bao, A. Klein-Hoffmann, G. Weinberg, D. Su and R. Schlögl, *J. Am. Chem. Soc.*, 2004, **126**, 7440–7441.
- 19 V. B. Fenelonov, V. N. Romannikov and A. Y. Derevyankin, *Microporous Mesoporous Mater.*, 1999, **28**, 57–72.
- 20 P. L. Llewellyn, Y. Grillet, F. Schuth, H. Reichert and K. K. Unger, *Microporous Mater.*, 1994, **3**, 2–6.
- 21 F. Di Renzo, A. Galarneau, D. Desplandier and F. Fajula, *Catal. Today*, 2001, **66**, 75–79.
- 22 E. C. De Oliveira, C. T. G. V. M. T. Pires and H. O. Pastore, *J. Braz. Chem. Soc.*, 2006, **17**, 16–29.

- 23 L. X. Xu, C. H. He, M. Q. Zhu, K. J. Wu and Y. L. Lai, *Catal. Letters*, 2007, **118**, 248–253.
- 24 E. B. Celer, M. Kruk, Y. Zuzek and M. Jaroniec, *J. Mater. Chem.*, 2006, **16**, 2824–2833.
- 25 H. Kotze and Immobilized Ru(II) Catalysts for Transfer Hydrogenation and Oxidative Alkene Cleavage Reactions, Ph.D. Thesis, Stellenbosch University, 2015.
- 26 R. E. Connick and C. R. Hurley, *J. Am. Chem. Soc.*, 1952, **74**, 5012–5015.
- 27 Y. Zhang, B. You, W. Hsu, C. Ren, X. Li and J. Wang, *Chem. Soc. Rev. Chem. Soc. Rev.*, 2015, **44**, 315–335.
- 28 M. M. Van Schooneveld, E. Vucic, R. Koole, Y. Zhou, J. Stocks, D. P. Cormode, C. Y. Tang, R. E. Gordon, K. Nicolay, A. Meijerink, Z. A. Fayad and W. J. M. Mulder, *Nano Lett.*, 2008, **8**, 2517–2525.
- 29 V. Ambrogio, F. Famiani, L. Perioli, F. Marmottini, I. Di Cunzolo and C. Rossi, *Microporous Mesoporous Mater.*, 2006, **96**, 177–183.
- 30 B. M. Bhanage and M. Arai, *Catal. Rev.*, 2001, **43**, 315–344.
- 31 J. H. Clark and D. J. Macquarrie, 1998, 853–860.
- 32 T. A. Heinrich, G. Von Poelhsitz, R. I. Reis, E. E. Castellano, A. Neves, M. Lanznaster, S. P. Machado, A. A. Batista and C. M. Costa-neto, *Eur. J. Med. Chem.*, 2011, **46**, 3616–3622.
- 33 C. L. Crawford, M. J. Barnes, R. A. Peterson, W. R. Wilmarth and M. L. Hyder, 1999, **581**, 194–206.
- 34 J. Mei, D. B. Pardue, S. E. Kalman, T. B. Gunnoe, T. R. Cundari, and M. Sabat, 2014, **33**, *Organometallics*, 5597–5605
- 35 D. B. Pardue, J. Mei, T. R. Cundari and T. Brent Gunroe, *Inorg. Chem.* 2014, **53**, 2968–2975

Figure captions

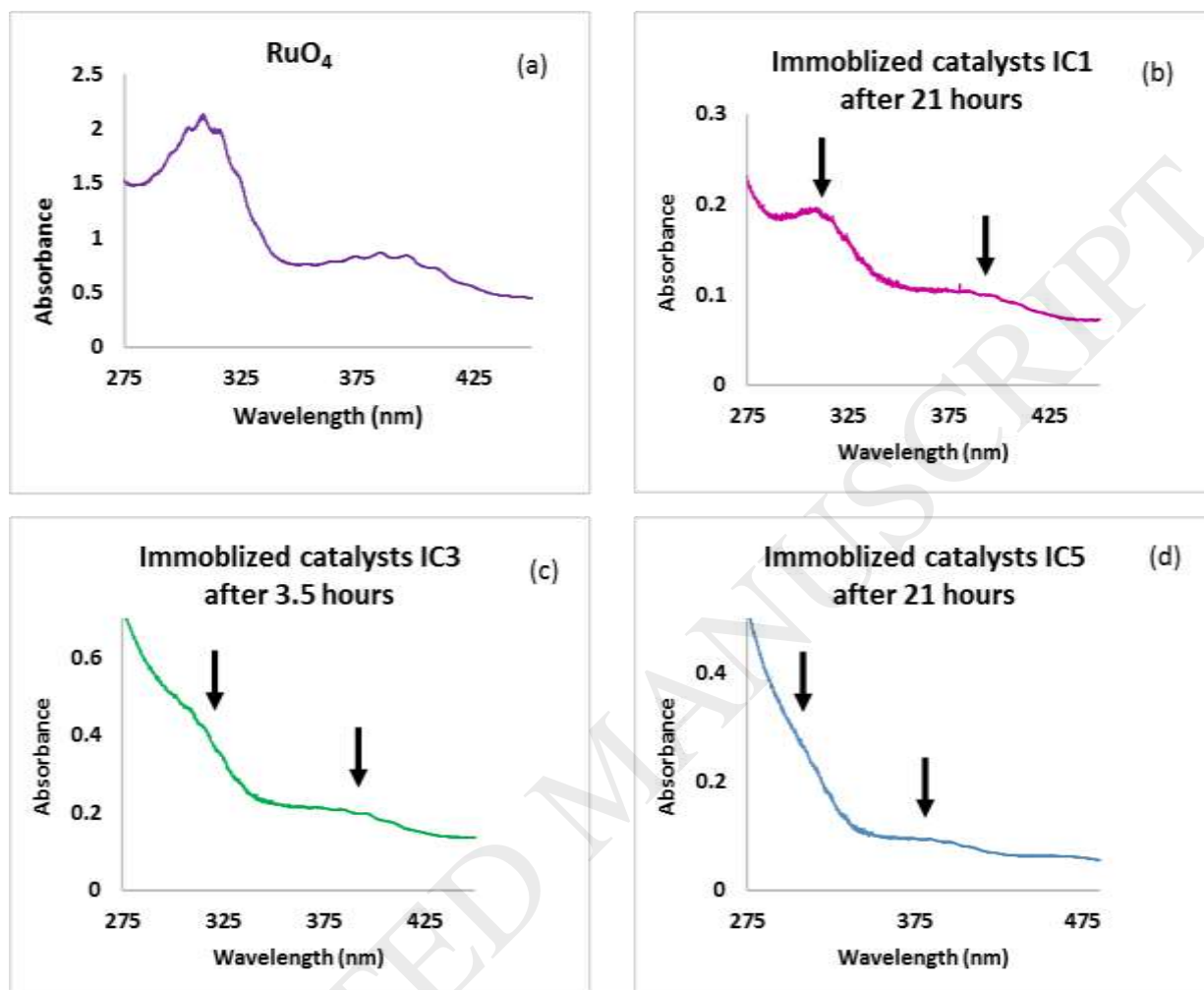


Figure 1: The UV-Vis spectrum indicating the formation of RuO₄ in organic layer of reaction mixtures using various ruthenium precursors (a) RuCl₃·xH₂O (b) IC1 (c) IC3 and (d) IC5

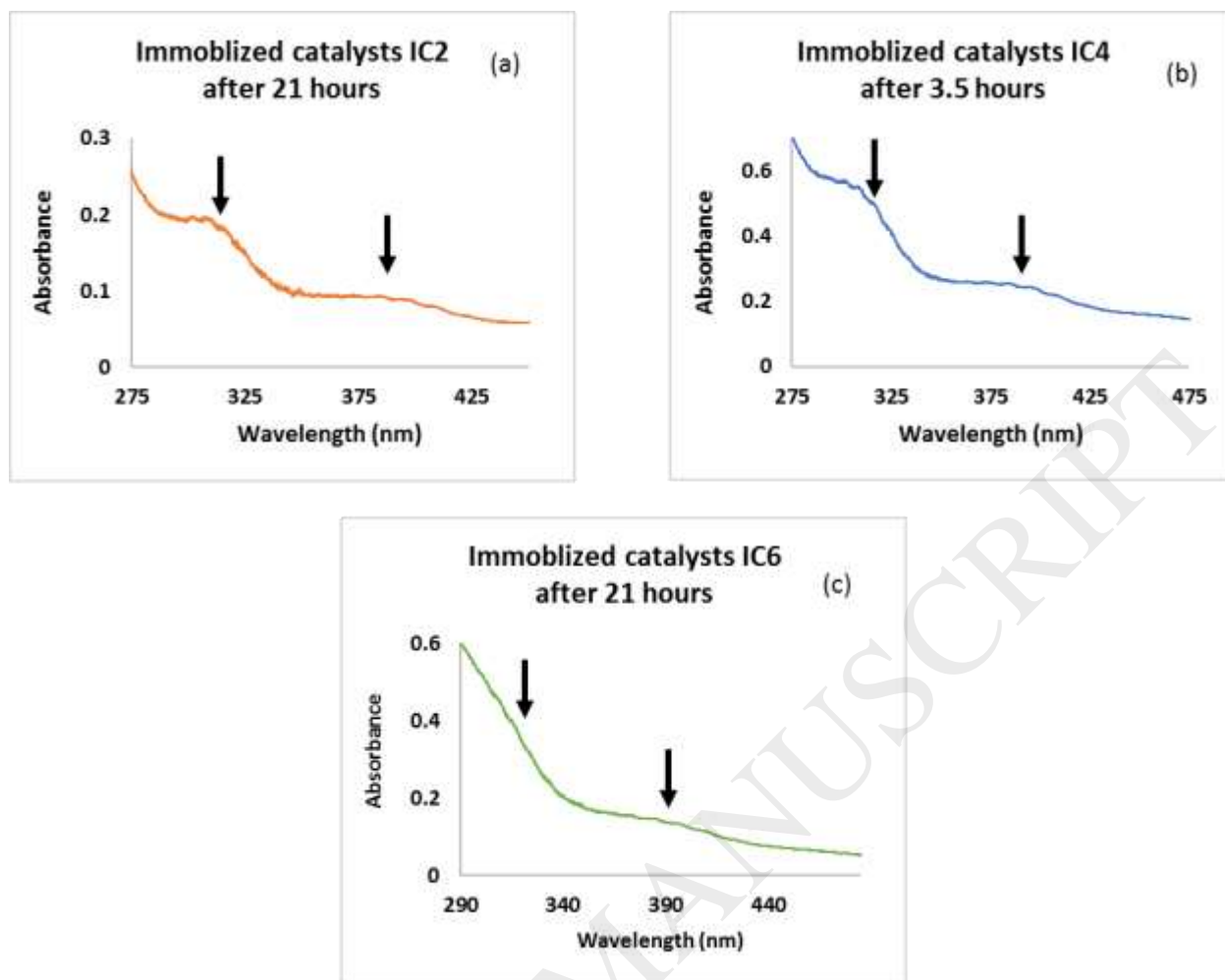


Figure 2 The UV-Vis spectrum indicating the formation of RuO_4 in organic layer of reaction mixtures using various ruthenium precursors (a) **IC3** (c) **IC4** and (d) **IC6**



Figure 3: Depiction of hydrophilic silica in the aqueous phase of biphasic solvent mixtures (1 = MCM-41 + H_2O /Ether; 2 = Model complex MC1 + CCl_4 /MeCN/ H_2O ; 3 = Immobilized complex IC1 + CCl_4 /MeCN/ H_2O ; 4 = MCM-41 + CCl_4 /MeCN/ H_2O).

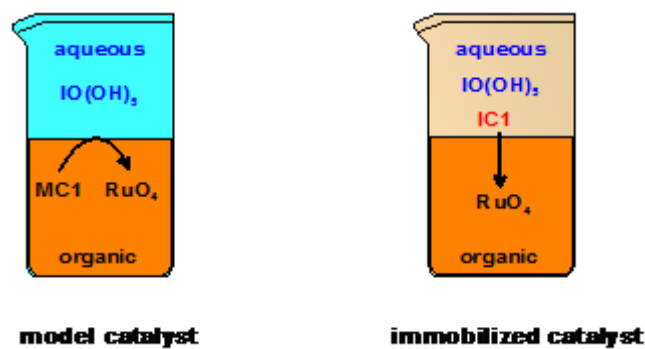


Figure 4: Depiction of the formation of RuO_4 from immobilized catalysts (left) versus model catalyst systems (right).

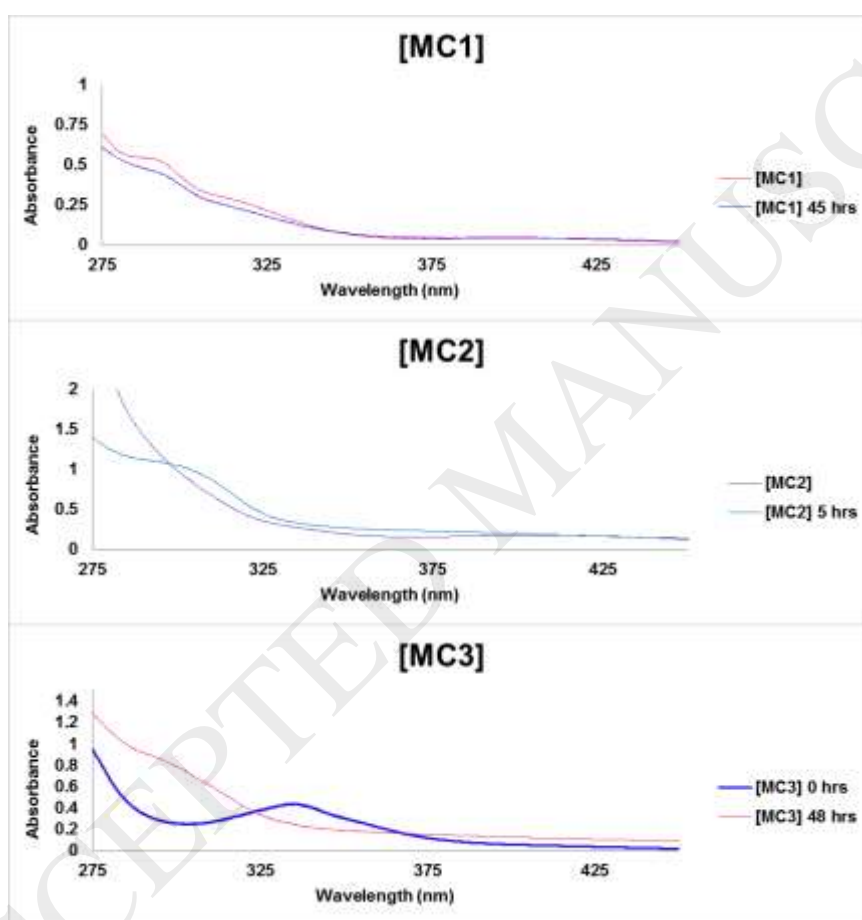


Figure 5: UV-Vis spectra of the organic layer of reaction mixtures using model catalysts, MC1-MC3.

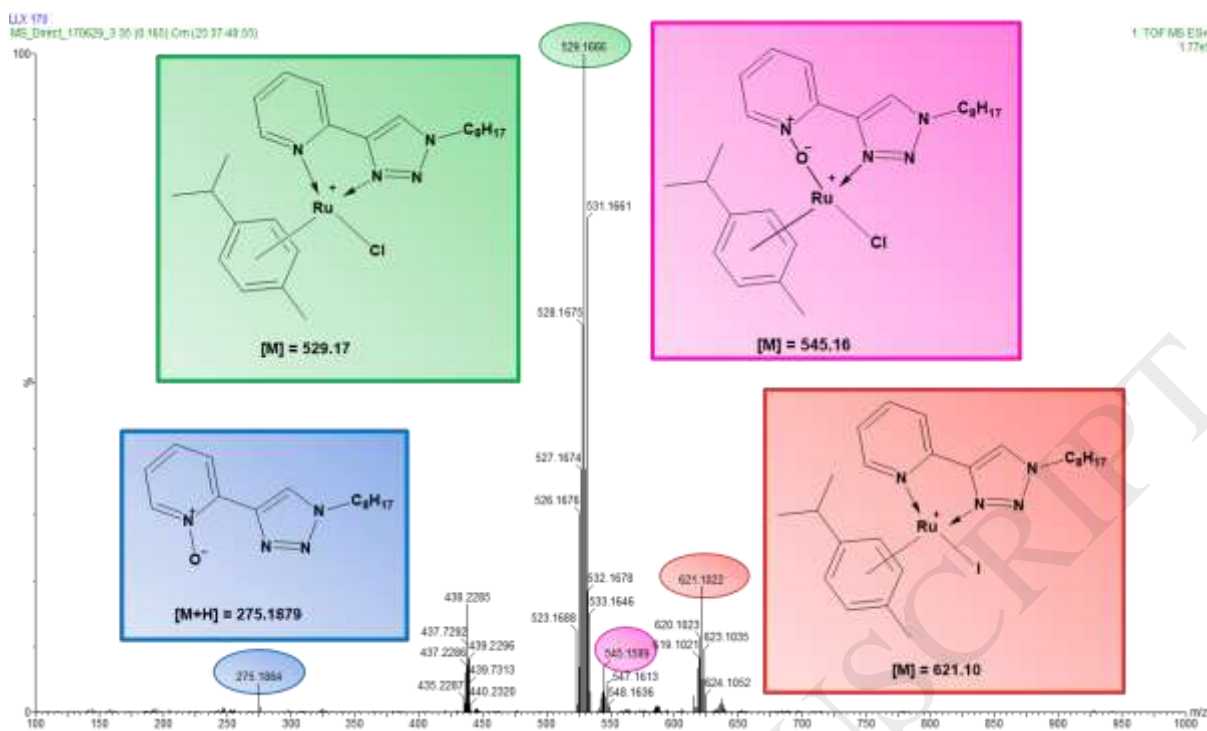
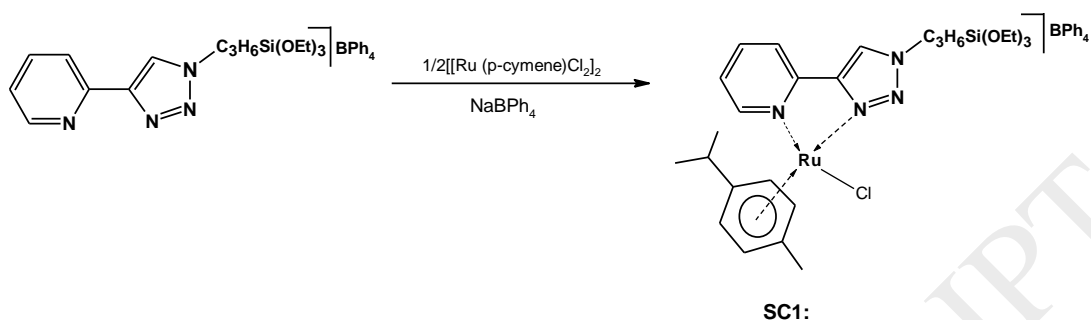
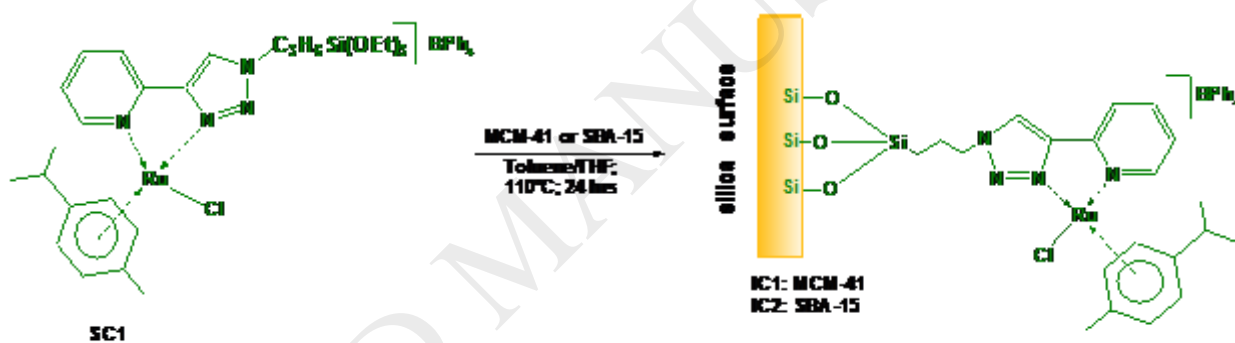


Figure 6: ESI-MS (positive mode) spectrum of model complex MC2 after reaction with 5 mol eqvs. IO(OH)₅.

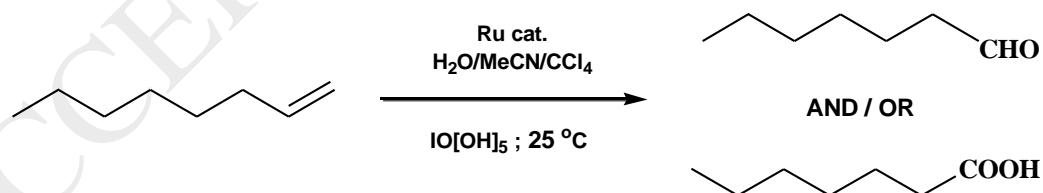
Scheme captions



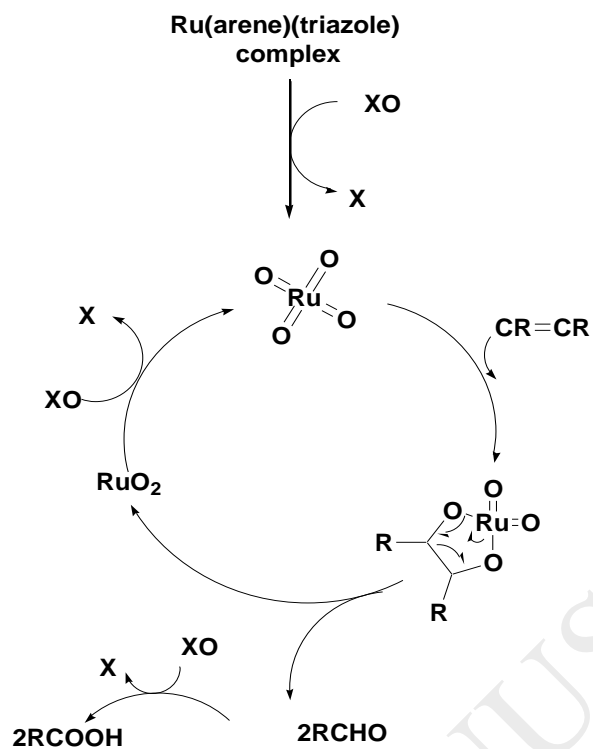
Scheme 1: Preparation of siloxane-functionalized complex, SC1



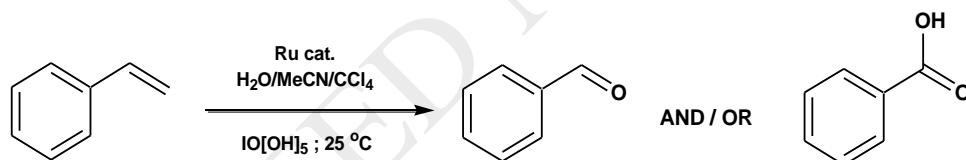
Scheme 2: Immobilization of siloxane-functionalized complex, SC1 on various types of silica



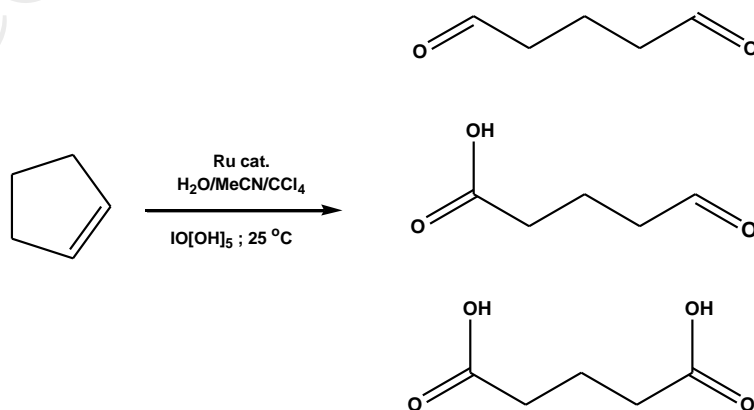
Scheme 3: Typical reaction conditions and products formed in the oxidative cleavage of 1-octene.



Scheme 4: Proposed mechanism for the oxidative cleavage of alkenes using a Ru(arene)(triazole) complex [25].



Scheme 5: Typical reaction conditions and products formed in the oxidative cleavage of styrene.



Scheme 6: Typical reaction conditions and products formed in the oxidative cleavage of cyclopentene.

ACCEPTED MANUSCRIPT

Chart

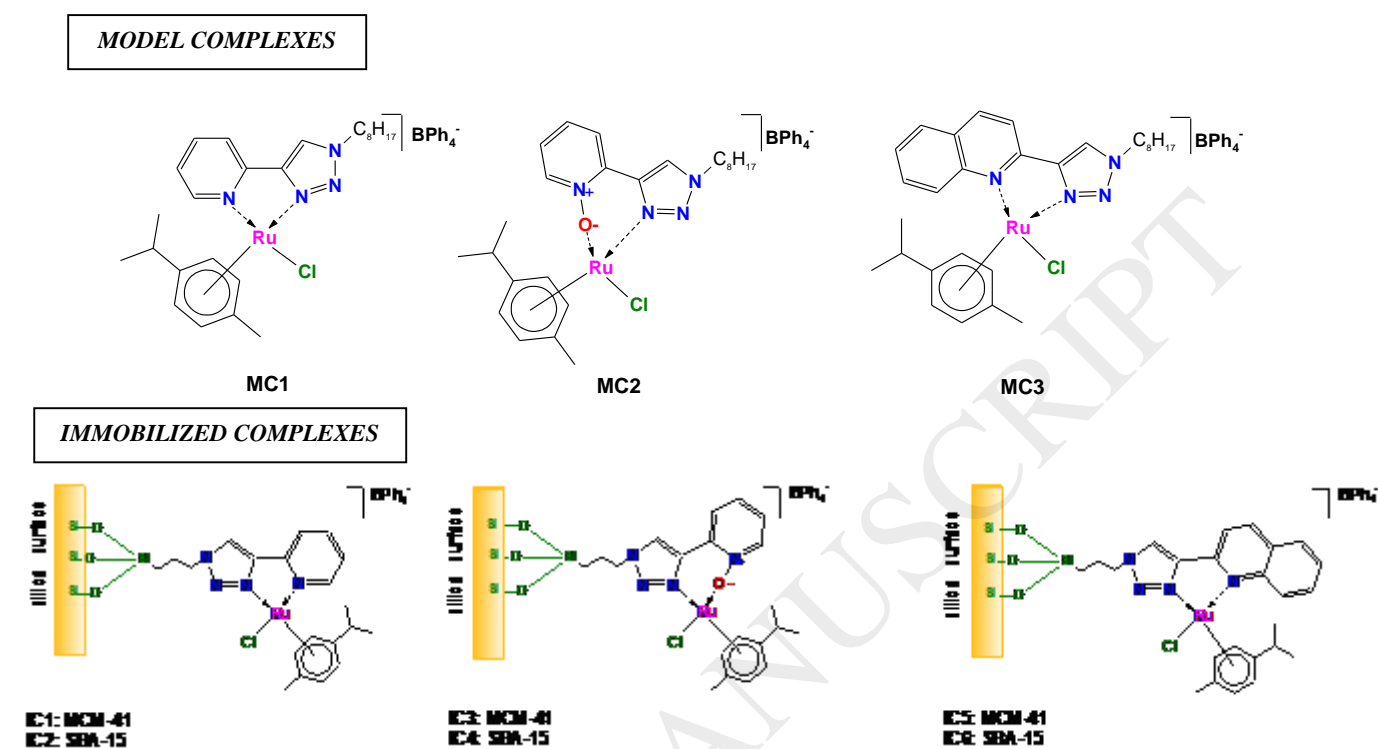


Chart 1: Catalyst precursors employed in the oxidative cleavage of alkenes.

Table

Table 1: Summary of BET surface area, average pore diameter and total pore volume of immobilized catalysts IC1-IC6

Material ^a	BET Surface Area (m ² /g)	Pore Diameter (Å)	Total Pore Volume (cm ³ /g)
MCM-41	1079	28.6	0.77
IC1 (MCM-41)	1 058	26.1	0.69
IC3 (MCM-41)	1 043	27.4	0.72
IC5 (MCM-41)	1 041	27.2	0.71
SBA-15	708	40.6	0.72
IC2 (SBA-15)	568	43.8	0.62
IC4 (SBA-15)	567	42.3	0.60
IC6 (SBA-15)	575	42.0	0.61

^a Support material indicated in brackets confirmed by TEM-EDS.

Table 2: Conversion of 1-octene and turnover numbers (TON) and turnover frequencies (TOF) obtained for catalysts evaluated in the oxidative cleavage of 1-octene.^a

Entry	Catalyst	Support material	Reaction time (hours)	Conversion ^b (%)	CHO/COOH ^c (%)	TON ^d	TOF ^e
1	MC1	N/A	3	4.80 ± 0.20	100/0	48	16.0
2	MC1	N/A	12	6.76 ± 1.86	100/0	68	5.6
3	IC1	MCM-41	3	28.5 ± 5.03	100/0	285	95.0
4	IC1	MCM-41	9	84 ± 2.80	73/13	840	93.3
5	IC2	SBA-15	3	34.3 ± 1.98	100/0	343	114.3
6	IC2	SBA-15	9	99.0 ± 2.10	51/48	990	110.0
7	MC2	N/A	3	25.0 ± 1.09	100/0	250	83.3
8	MC2	N/A	6	100 ± 1.29	29/71	1000	166.7
9	IC3	MCM-41	3	46.8 ± 5.46	89/11	468	156.0
10	IC3	MCM-41	6	100 ± 1.20	0/100	1000	166.7
11	IC4	SBA-15	3	50.4 ± 4.62	92/4	504	168.0
12	IC4	SBA-15	6	100 ± 1.79	0/100	1000	166.7
13	MC3	N/A	3	9.20 ± 2.50	100/0	920	30.7
14	MC3	N/A	12	24.1 ± 1.54	100/0	241	20.1
15	IC5	MCM-41	3	23.8 ± 1.79	100/0	238	79.3

16	IC5	MCM-41	9	100± 1.19	80/20	1000	111.1
17	IC6	SBA-15	3	27.0 ± 4.20	100/0	270	90.0
18	IC6	SBA-15	9	90.0 ± 1.60	83/17	900	100.0

[a] Reaction conditions: 1-octene (0.5 mmol); IO(OH)₅, (2.5 mmol); 25 °C; 0.1 mol% Ru catalyst loading [b] 1-octene consumption. This is the average of at least two runs. [c] % heptaldehyde vs. heptanoic acid formed [d] TON = mmol octene consumed /mmol catalysts [e] TOF = mmol octene consumed/mmole catalyst/hour

Table 3: Oxidative cleavage of other alkenes with immobilized catalyst, IC4.^[a]

Entry	Substrate	Time (hrs)	Substrate conv. (%)	Products (Selectivity %)
1	Styrene	0.5	100	Benzaldehyde (100)
2	Styrene	1	100	Benzaldehyde (93.4) Benzoic acid (6.6)
3	Cyclopentene	0.5	100	Glutaraldehyde
4	Cyclopentene	1	100	Glutaraldehyde (37.7%), 5-hydroxypentanoic acid (47.3%) and glutaric acid (15.0%)
5	1-octene	3	50	Heptaldehyde (91.7) Heptanoic acid (8.3)

[a] Reaction conditions: Water (2.5 mL), CCl₄ (1.25 mL) and MeCN (1.25 mL); 1-octene (0.5 mmol); IO(OH)₅, (2.5 mmol); 25 °C; 0.1 mol% Ru catalyst loading